TENSILE BEHAVIOR OF T-STUB SUBJECTED TO STATIC AND DYNAMIC LOADS

Hao Huang [1], Lu-Ming Ren [1], Kang Chen [1], Xiu-Jiang Li [2], Lin Wang[3] and Bo Yang [1]*

[1] School of Civil Engineering, Chongqing University, Chongqing 400045, China
E-mails: 201916021033@cqu.edu.cn, renlm@cqu.edu.cn, chen0429@cqu.edu.cn, yang0206@cqu.edu.cn

[2] Chongqing Monorail Transit Engineering Co. Ltd, Chongqing 400081, China
E-mail: 179798594@qq.com

[3]Citic Heavy Industries Co. LTD, Henan 471039, China
E-mail: wl6286200@163.com

Abstract: *To study the tensile behavior of T-stubs with various design parameters under different loading scenarios, uniaxial static and dynamic tensile tests were carried out. The effects of flange thickness, bolt preload, bolt strength and loading conditions were discussed. The failure modes observed under different conditions were presented. Besides, the load-displacement response was analyzed in detail. The experimental results showed that the bolt preload only affected the initial stiffness of the specimens, and smaller flange thickness and lower bolt strength would result in unfavorable performance of T-stubs. Under dynamic loading scenarios, the test specimens showed greater resistance but limited deformation capacity compared to the static ones. Furthermore, it was observed that the ductility would be seriously reduced if brittle failure, such as bolt or weld fracture occurred which is recommended to be avoided in structural design.*

Keywords: T-stub; Tensile behavior; Static and dynamic test; Failure mode

DOI: 10.18057/ICASS2020.P.313

1 INTRODUCTION

Design of beam-column connections in steel structures is crucial to effectively resisting applied loads. The steel connections mainly include rigid, semi-rigid and simple connections. Semi-rigid connections are widely used in practice because of their advantages including strong plastic deformation capacity, convenient installation, clear force transmission and etc. At present, bolted end plate connections are one of the most popular semi-rigid connection types recommended by many steel structure specifications.

Equivalent T-stub is an essential mechanical component of the end plate connections. The current European Code for the design of steel structures (EN 1993-1-8:2004[1]) recommends a component-based modeling approach for steel connection design. Since the component-based method was introduced into EC3 in 1992, it has been widely used to study different mechanical behaviors of steel connections. The fundamental process is mainly divided into three steps: (1) Splitting the connection and determining the equivalent size of effective mechanical components; (2) Analyzing the mechanical behavior (stiffness, load-bearing capacity) of each component; (3) Combining the initial stiffness and load-bearing capacity of all the components to obtain those properties of the whole connection.

In recent years, with the development component-based modeling approach, it has been gradually used in different connection types and loading conditions. Swanson et al. [2,3] and Coelho et al. [4,5] carried out uniaxial static tensile tests on T-stubs with various design parameters such as section size, bolt diameter, hole spacing and they pointed out the influence of different design parameters on the mechanical properties of T-stubs. Piluso et al. [6,7] confirmed three failure modes of T-stubs through static tensile tests and proposed a four-fold line model for predicting the load-displacement response. Besides the tests carried out at room temperature, some high-temperature tests about the component-based modeling approach have also been conducted by Both et al. [8]. They determined the relationship between temperature and mechanical properties of components through test results. Ribeiro et al. [9,10] investigated the influence of dynamic load on T-stubs through a novel device and found that loading time was critical to T-stub performance. Zhao et al. [11] proposed a correction factor for EC3, which can accurately predict the design plastic bearing capacity of the T-stub made of S690 steel.

With the continuous development of the steel connections, research on their basic components also gradually developed. In the past few decades, most of the mechanical properties of the components have been studied under monotonic, static and cyclic loading conditions. Many researchers have proposed suggestions to improve the current standards, but there is little information about the mechanical properties of components under dynamic load. The comparison between the dynamic and static conditions is even less. However, the connections are often damaged by dynamic loads when the structure is subjected to accidental loads, such as fire, explosion, impact and etc. Thus, this paper intends to investigate mechanical properties of component T-stub under dynamic load emphasizing on the difference of static and dynamic loading conditions. T-stubs with different design parameters were tested by a static tensile testing machine, while corresponding specimens were tested by a novel dynamic apparatus. Both the load-displacement curves and failure modes of the test specimens were presented. Specifically, the initial stiffness, load resistance and plastic stage behavior were analyzed.

2 TEST METHODOLOGY

In this test, the T-stub specimen was taken from the extended end plate connection of a typical 6-story steel frame commercial building, as shown in Figure 1.

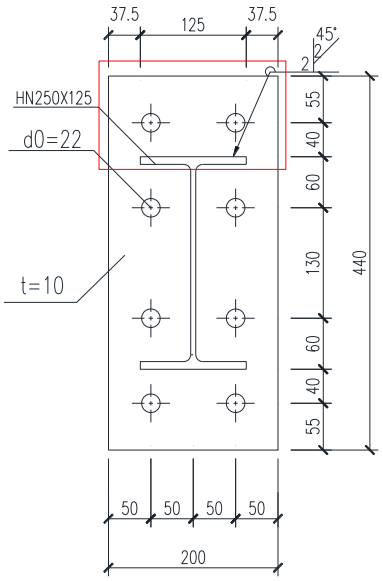

Figure 1: Extended end plate connection of the prototype structure

2.1 Static test

In order to study the influence of different design parameters on the mechanical properties of T-stubs, 5 groups of test specimens were designed, as shown in Figure 2. The detailed design parameters are shown in Table 1, where t_f is the flange thickness and P is the bolt preload. The web and flange of T-stubs were made of Q355 hot-rolled steel plate. Fillet welds of 8mm thickness were used to connect and flange. The diameters of all the bolts used in the T-stubs were 20mm. The material properties of steels and bolts are given in Tables 2 and 3.

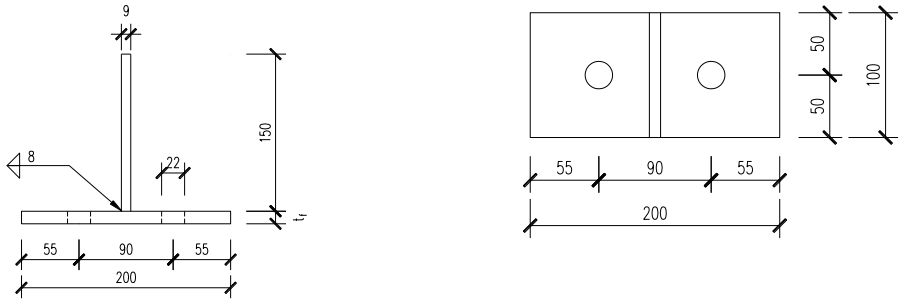

(a) Front view (b) Top view

Figure 2: Geometry characteristics of a T-stub in static tests

Table 1: Design parameters of specimens in static tests

Specimen	t_f(mm)	Bolt grade	P(kN)
S-F12-B10.9-P150	12	10.9S	150
S-F10-B10.9-P150	10	10.9S	150
S-F12-B10.9-P0	12	10.9S	150
S-F12-B8.8-P125	12	8.8	125
S-F12-B12.9-P175	12	12.9	175

Table 2: Mechanical properties of steels

Sample location	Thickness T(mm)	Elastic modulus E(GPa)	Yield stress f_y(MPa)	Ultimate stress f_u(MPa)	Tensile elongation (%)
Beam flange	9	206	359	525	35
End plate	10	207	370	502	38
End plate	12	205	388	487	33
End plate	14	210	384	533	33.5

Table 3: Mechanical properties of high-strength bolts

Steel grade	Yield stressf_y(MPa)	Ultimate stress f_u(MPa)	Tensile strain ε_u
8.8	711	867	0.14
10.9S	1140	1216	0.12
12.9	1152	1306	0.12

The quasi-static tests of T-stubs were carried out on a 60t testing machine at Chongqing University, as shown in Figure 3. In the test, it was assumed that the other side of the test specimen was a rigid body. Thus, a thick T-stub was designed to ensure that it would not deform during the whole loading process, which was also used in the dynamic test. The testing machine could clamp the web of the test specimen through the fixture. During installation, the test

specimens were vertically centered to ensure that the two webs were aligned in the same straight line.

(a) Testing machine (b) Test setup

Figure 3: Static test setup

The test process was divided into two stages. The first stage was preloading: after arranging all instrumentations, applying a tensile force of 10% yield load to the test specimen and then reducing it to zero, ensuring the measured data changed linearly. The second stage was formal loading: the displacement control loading was applied on the test specimen until the specimen totally failed, for instance flange fracture and bolt failure occurred. The displacement of the rigid T-stub was measured by dial indicators, which were used to represent the flange deformation. The tensile force could be recorded by the testing machine.

2.2 Dynamic test

Five groups of dynamic specimens were designed to be compared with the static test. The geometry characteristics of T-stubs are shown in Figure 4, and the design parameters of various specimens are shown in Table 4,where t_f is the flange thickness and P is the bolt preload.

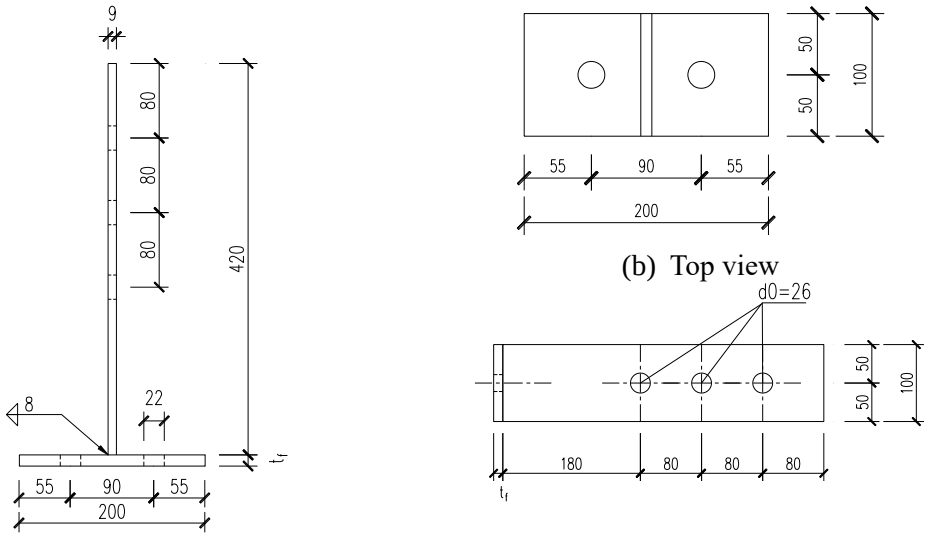

(a) Front view (b) Top view (c) Side view

Figure 4: Geometry characteristics of a T-stub in dynamic tests

Table 4: Design parameters of specimens in dynamic tests

Specimen	t_f(mm)	Bolt grade	P(kN)

D-F12-B10.9-P150	12	10.9S	150
D-F10-B10.9-P150	10	10.9S	150
D-F12-B10.9-P0	12	10.9S	150
D-F12-B8.8-P125	12	8.8	125
D-F12-B12.9-P175	12	12.9	175

The static tensile test machine was not applicable for the dynamic test so that a novel dynamic loading device was designed as shown in Figure 5. Different from the static test specimens, the webs of T-stubs were lengthened, and three screw holes were drilled on them to connect with the loading device.

Before the test, the hand chain block was used to pull the clump weight from the ground to the design falling height. Then two electromagnets were placed at the adsorption position corresponding to the clump weight and energized. At this time, the clump weight had been sucked up by the electromagnet through the magnetic force, so the hand chain block could be removed carefully. After installing all the measuring equipment, the electromagnet was turned off so that the clump weight began to fall freely after losing magnetic adsorption. The gravitational potential energy was converted into kinetic energy. When the clump weight passed the designed falling height, the steel wire rope bore force. Meanwhile, the kinetic energy of the clump weight was transferred to the specimen at the other end to achieve the effect of dynamic load. In the test, the falling height was 3m and the mass of the clump weight was 800kg. The vertical load and displacement of the thick T-stub were measured by the load sensors and laser displacement sensors, respectively

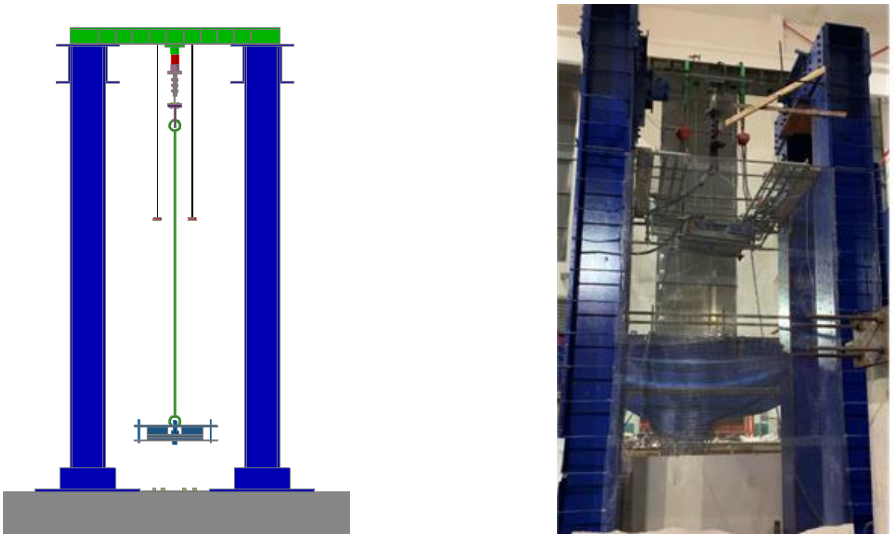

(a) Schematic diagram (b) Loading device

Figure 5: Dynamic test setup

For the sake of safety, rubber pads and wood beams were placed on the ground below the clump weight, avoiding the clump weight or the test T-stub falling off accidentally. Another safety steel wire rope was also set to connect the end of the rigid T-stub to prevent it from falling off the ground after the failure of the test specimen.

3 TEST RESULT

3.1 Failure modes

Owing to the different design parameters and load forms, the test T-stubs showed various failure modes. In the static group, specimen S-F12-B10.9-P150 failed in a mixed mode, that is

yield failure near the weld toe accompanied by bolt fracture, as illustrated in Figure 6a. Yield failure of flange near weld toe and bolt hole was observed for specimen S-F10-B10.9-P150, as shown in Figure 6b. Specimen S-F12-B10.9-P0 showed the same failure mode as specimen S-F12-B10.9-P150 (see Figure 6c). Micro yield cracking at the weld toe with bolt fracture were observed for both specimen S-F12-B8.8-P125 and specimen S-F12-B12.9-P175 as shown in Figures 6d and 6e. In the dynamic group, specimen D-F12-B10.9-P150 was not completely damaged after the first loading, but obvious weld toe yielding and bolt bending deformation were observed (Figure 6f). For specimen D-F10-B10.9-P150, the bolts deformed slightly, while the weld toe and flange near the bolt hole had severe yield failure, as shown in Figure 6g. The nut sliding thread occurred in specimen D-F12-B10.9-P0 (see Figure 6h), which is unconventional damage and should be avoided. Failure modes of specimens D-F12-B8.8-P125 and D-F12-B12.9-P175 were bolt failure, as shown in Figures 6i and 6j.

(a) Specimen S-F12-B10.9-P150, a mixed mode

(b) Specimen S-F10-B10.9-P150, flange fracture

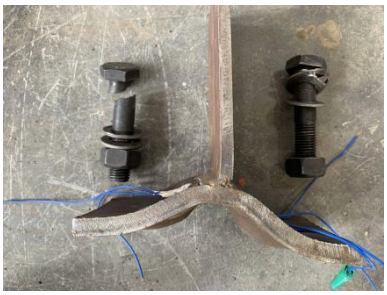

(c) Specimen S-F12-B10.9-P0, a mixed mode

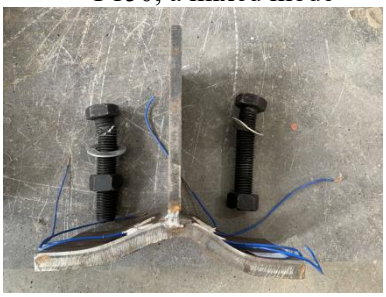

(d) Specimen S-F12-B8.8-P125, bolt fracture

(e) Specimen S-F12-B12.9-P175, bolt fracture

(f) Specimen D-F12-B10.9-P150, Undamaged

(g) Specimen D-F10-B10.9-P150, flange fracture

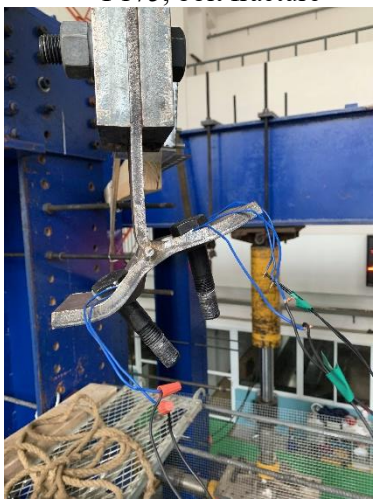

(h) Specimen D-F12-B10.9-P0, stripping of the nut

(i) Specimen D-F12-B8.8-P125, bolt fracture

threads

(j) Specimen D-F12-B12.9-P175, bolt fracture

Figure 6: Failure modes

3.2 Load-displacement characteristic

Figure 7 shows the load-displacement curves under static and dynamic conditions and the comparison between them.

In the static test, it can be seen that the applied preload had little effect on the peak load and ultimate displacement. The maximum load of specimen S-F12-B10.9-P150 was 420kN, 0.007% lower than the one without preload. One bolt of specimens S-F12-B10.9-P150 and S-F12-B10.9-P0 fractured when the displacement reached 36.8mm and 39mm, respectively, with a difference of 6%. Nevertheless, a significant reduction in initial stiffness was observed if the preload was not applied. Reducing the flange thickness not only changed the failure mode but also decreased the maximum load-bearing capacity and ductility. The maximum load and displacement of specimen S-F10-B10.9-P150 were 297kN and 27mm, 41% and 36% lower than that of specimen S-F12-B10.9-P150, respectively. Similarly, the maximum load of specimen S-F12-B8.8-P125 was 291kN, 44.3% lower than that of specimen S-F12-B10.9-P150, which adopted 10.9S high strength bolts. The ultimate displacement of specimen S-F12-B8.8-P125 was 30mm, which was also 22.7% smaller compared with specimen S-F12-B10.9-P150. It is worth noting that the load-displacement curve of specimen S-F12-B12.9-P175 was not as high as expected, and the maximum load was 334kN, 25.7% less than specimen S-F12-B10.9-P150. Besides, the ultimate displacement was only 20.8 mm for this specimen, 77% less than that of specimen S-F12-B10.9-P150.

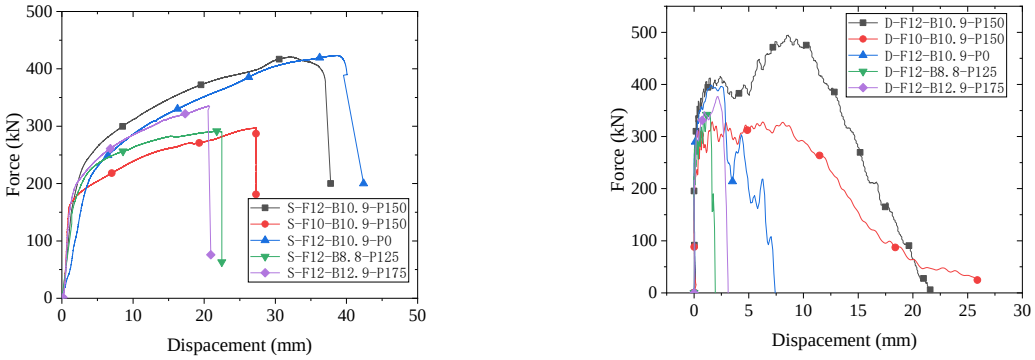

(a) Static tests (b) Dynamic tests

Figure 7: Load-displacement curves

In dynamic tests, each specimen had experienced one impact except for specimen D-F12-B10.9-P150, which did not fail completely after the first impact. It can be seen from Figure 7 that the specimens without bolt fracture had better ductility and could absorb more energy. The occurrence of bolt fracture seriously reduced the deformation capacity of T-stubs. Besides, specimens with bolt fracture reached the ultimate displacement at the maximum force. However,

the same phenomenon was not observed in the specimens with flange failure. The maximum load of specimen D-F12-B10.9-P150 was 494kN, 33.6% larger than that of specimen 2-F10 (328kN). Meanwhile, the peak load of test specimens D-F12-B8.8-P125 and D-F12-B12.9-P175 were 346kN and 376kN, respectively, 42.8% and 23.4% less than that of specimen D-F12-B10.9-P150.

Through the comparison of the load-displacement curves of dynamic and static tests (since D-F12-B10.9-P0 showed an abnormal failure mode, it was not included in the comparison), it was obvious that the impact action resulted in a significant improvement of the initial stiffness of the specimen. If the bolt did not fail prematurely, the maximum load in the dynamic test appeared before the limit displacement, which was entirely different from the static test. The maximum loads of specimens D-F12-B10.9-P150, D-F10-B10.9-P150, D-F12-B8.8-P125 and D-F12-B12.9-P175 were 15%, 9.8%, 15.9% and 11.1% higher than that of corresponding static test specimens, respectively. In completely destroyed specimens, the ultimate displacement of specimen D-F10-B10.9-P150 with flange failure was 26mm, 10% different from that of specimen S-F10-B10.9-P150. Specimens D-F12-B8.8-P125 and D-F12-B12.9-P175 had the ultimate displacements of 2mm and 3.1mm, respectively, which were 1400% and 500% smaller than the corresponding static ones.

4 CONCLUSION

Based on two different loading methods (static and dynamic loading), the axial tensile behavior of T-stubs with various design parameters was studied, and the following conclusions can be drawn:

(1) In the static test, bolt fracture should be avoided until the deformation of the flange developed sufficiently. Preload could improve the initial stiffness of the specimen, but did not affect the ultimate resistance and displacement.

(2) In the dynamic test, it was observed that the energy absorption capacity of T-stubs would be seriously reduced if weld or bolt damage occurred. Thus, these two failure modes should be avoided in practice.

(3) The test T-stubs showed higher load-bearing capacity under dynamic load, but the ductility had been severely weakened. In addition, failure of specimens under static loading required more energy than that of dynamic ones, which indicated that the dynamic effect would weaken the tensile behavior of the specimen.

ACKONWLEDGMENTS

This work is supported by Development of hydraulic pile hammer for offshore operation under Project MC-202014-S01.

REFERENCES

[1] Eurocode 3, Part 1-8 (EC3-1-8), Design of steel structures-Part 1-8: Design of joints, UK, British Standards Institution, 2004.

[2] Swanson J.A. and Leon R.T. L., “Bolted Steel Connections: Tests on T-Stub Components”, *Journal of Structural Engineering*, 126(1), 50-56, 2000.

[3] Swanson J.A. and Leon R.T., “Stiffness Modeling of Bolted T-Stub Connection Components”, *Journal of Structural Engineering*, 127(5), 498-505, 2001.

[4] Coelho A. M. G., Bijlaard F., and Gresnigt N., "Experimental assessment of the behaviour of bolted T-stub connections made up of welded plates", *Journal of Constructional Steel Research*, 60(2), 269-311, 2004.

[5] Coelho A. M. G., Silva L., and Bijlaard F. S. K., "Finite-element modeling of the nonlinear behavior of bolted T-stub connections", *Journal of Structural Engineering*, 132(6), 918-928, 2006.

[6] Piluso V., Faella C. and Rizzano G., "Ultimate behavior of bolted T-stubs. I: Theoretical model", *Journal of Structural Engineering*, 127(6), 686-693, 2001.

[7] Piluso V., Faella C. and Rizzano G., "Ultimate Behavior of Bolted T-Stubs. II: Model Validation", *Journal of Structural Engineering*, 127(6), 694-704, 2001.

[8] Both I., Duma D. and Dinu F., "The influence of loading rate on the ultimate capacity of bolted T-stubs at ambient and high temperature", *Fire Safety Journal*, 125, 103438, 2021.

[9] Ribeiro J., Santiago A. and Rigueiro C., "Material modelling of tensile steel component under impulsive loading", *International Conference on Vibration Problems*, 2014.

[10] Ribeiro J., Santiago A. and Rigueiro C., "Numerical assessment of T-stub component subjected to impact loading", *Engineering Structures*, 106, 450-460, 2016.

[11] Zhao M. S., Lee C. K. and Chiew S. P., "Tensile behavior of high performance structural steel T-stub joints", *Journal of Constructional Steel Research*, 122, 316-325, 2016.